

# First-principles calculation of charged capacitors under open-circuit conditions using the orbital-separation approach

Shusuke Kasamatsu,<sup>1,\*</sup> Satoshi Watanabe,<sup>2</sup> and Seungwu Han<sup>3,†</sup>

<sup>1</sup>*The Institute for Solid State Physics, The University of Tokyo, 5-1-5 Kashiwanoha, Kashiwa-shi, Chiba 277-8581, Japan*

<sup>2</sup>*Department of Materials Engineering, The University of Tokyo, 7-3-1 Hongo, Bunkyo-ku, Tokyo 113-8656, Japan*

<sup>3</sup>*Department of Materials Science and Engineering and Research Institute of Advanced Materials, Seoul National University, Seoul 151-742, Korea*

(Received 16 March 2015; revised manuscript received 29 June 2015; published 11 September 2015)

In a previous work [Phys. Rev. B **84**, 085120 (2011)], we presented the orbital-separation approach for simulating metal/insulator/metal capacitors under bias voltage within the Kohn-Sham framework of density functional theory. A limitation mentioned in that work was that it is not straightforward to calculate the amount of free charge transferred from one electrode to the other, and thus the application of the method was limited to the closed-circuit (constant-voltage) condition. Here, we show that it is actually possible in practice to calculate the free charge by examining the change in the occupation of the Kohn-Sham eigenstates near the Fermi level. Thus it is also possible to perform open-circuit (constant-charge) simulations, and we demonstrate this on a metal/ferroelectric/metal capacitor.

DOI: [10.1103/PhysRevB.92.115124](https://doi.org/10.1103/PhysRevB.92.115124)

PACS number(s): 71.15.-m, 73.40.Rw, 77.22.-d

## I. INTRODUCTION

The understanding and optimization of interface and surface properties of materials is imperative for further development of microelectronic devices, which have become an indispensable and integral part of modern-day society. The same applies to catalysis in electrochemical energy conversion and storage, whose importance is ever-increasing as we try to exploit renewable energy resources towards realizing a sustainable society.

To understand the properties and functions of interfaces/surfaces and to obtain materials design principles, first-principles simulation based on the Kohn-Sham (KS) formalism of density functional theory (DFT) [1,2] has been gaining popularity as a go-to method. Although the original KS formalism was limited to simulation of the electronic ground state, recent advances in simulation methodologies have made possible the simulation of nano structures under electrical bias, which is essential for probing the performance of nanodevices under operating conditions [3–12]. In this context, we previously proposed the *orbital-separation approach* (OSA), which is applicable to metal/insulator/metal capacitors of arbitrary geometries as long as there is negligible electronic current between the electrodes [13]. The method is based on the separation of Kohn-Sham eigenstates with energies near the Fermi level into each of the metal electrode parts, then occupying them according to the Fermi levels assigned to each of the electrodes. The Fermi levels are determined so that the system satisfies charge neutrality while maintaining a preset Fermi level difference (i.e., voltage between electrodes). The accuracy of the approach was also evaluated, and it was found that the OSA gives consistent quantities with that derived from density functional perturbation theory calculations of the dielectric constant in bulk systems; this suggests that errors would originate not from the approach itself, but from the

limitations of the functional approximations used in the KS procedure and insufficient convergence in the self-consistent field calculations. The main merits of this approach are its applicability to arbitrary electrode geometries and freedom of choice in the basis set expansion of the wave functions, as well as simplicity of implementation; a somewhat thorough discussion on the strengths and weaknesses of this approach in comparison with other finite-bias methods has been given in Ref. [13]. Although this made possible closed-circuit, constant-voltage simulations of metal/insulator/metal capacitors, we were unable to calculate the free charge transferred from electrode to electrode. One may first think that the free charge can be calculated from electron density differences, but this is actually not the case, as it is nontrivial to separate out the polarization charge from the free charge.

Calculation of the free charge is desirable for several reasons. One of them is that the variational quantity during a constant-voltage simulation is the grand potential that may be calculated as

$$\Omega = E_{\text{KS}} - VQ, \quad (1)$$

where  $E_{\text{KS}}$  is the Kohn-Sham total energy of the capacitor,  $V$  is the applied bias voltage, and  $Q$  is the free charge that is transferred from one electrode to the other due to the applied bias. Without knowledge of the free charge  $Q$ , it is not possible to calculate this quantity. This makes energy-based optimization methods for structural relaxation unusable, and we would also lack access to a conserved quantity for evaluation of the accuracy of molecular dynamics simulations (it should be noted, however, that the forces can be obtained without knowledge of the grand potential as shown in Ref. [13]). Another reason is that the ability to evaluate the free charge would make possible open-circuit (constant-charge) simulations, which is particularly useful for examining ferroelectric materials as pointed out in Ref. [14].

In this work, we show that we can actually calculate the free charge by comparing the occupation of the KS eigenstates near the Fermi level before and after bias application. Based on this

\*kasamatsu@issp.u-tokyo.ac.jp

†hansw@snu.ac.kr

idea, we implement a constant-charge version of the OSA and test its use on a ferroelectric capacitor.

## II. ORBITAL-SEPARATION APPROACH

We start with a short review of the orbital-separation approach (OSA) of Ref. [13]. In the conventional self-consistent-field (SCF) KS-DFT scheme, the charge density is constructed in each SCF step from the lowest-energy KS orbitals:

$$\rho(\mathbf{r}) = \sum_{\mathbf{k}} \sum_i w_{\mathbf{k}} f_{\sigma}(\epsilon_{i,\mathbf{k}} - \epsilon_{\text{F}}) |\psi_{i,\mathbf{k}}(\mathbf{r})|^2. \quad (2)$$

Here,  $i$  is the band index,  $\mathbf{k}$  stands for the  $\mathbf{k}$  points used in the Brillouin zone integration,  $w_{\mathbf{k}}$  is the  $\mathbf{k}$ -point weight,  $f_{\sigma}$  is the function used for smearing of the occupation numbers for faster convergence,  $\psi_{i,\mathbf{k}}$  is the KS orbital,  $\epsilon_{i,\mathbf{k}}$  is the eigenenergy of the KS orbital, and  $\epsilon_{\text{F}}$  is the Fermi level which is determined from charge conservation

$$\int_{\text{unit cell}} \rho(\mathbf{r}) d\mathbf{r} = N, \quad (3)$$

where  $N$  is the number of electrons in the unit cell. In the OSA, this occupation scheme is modified to simulate the effect of bias voltage. The basic idea stems from the fact that in a system consisting of metallic parts well separated by insulating parts, the KS orbitals near the Fermi level can be separated out into each of the metallic (electrode) parts because there are no eigenstates within the band gap of insulators. The separation can be performed in each SCF step by examining the spatial distribution of each KS orbital within a preset energy window around the Fermi level  $\epsilon_{\text{F}}$  determined from Eqs. (2) and (3). Once the separation is done, the occupation functions can be given as

$$f_{i,\mathbf{k}} = \begin{cases} 1, & \epsilon_{i,\mathbf{k}} < \epsilon_{\text{win}}^{\text{lower}}, \\ 0, & \epsilon_{i,\mathbf{k}} > \epsilon_{\text{win}}^{\text{upper}}, \\ f_{\sigma}(\epsilon_{i,\mathbf{k}} - \epsilon_{\text{F},\alpha(i,\mathbf{k})}), & \epsilon_{\text{win}}^{\text{lower}} \leq \epsilon_{i,\mathbf{k}} \leq \epsilon_{\text{win}}^{\text{upper}}, \end{cases} \quad (4)$$

where  $\epsilon_{\text{win}}^{\text{lower}}$  and  $\epsilon_{\text{win}}^{\text{upper}}$  are the lower and upper bounds of the energy window, and  $\alpha(i,\mathbf{k})$  specifies the electrode to which the KS orbital  $\psi_{i,\mathbf{k}}$  belongs. The Fermi levels in each electrode

$\epsilon_{\text{F},\alpha}$  are determined so as to maintain total charge neutrality

$$\int \rho(\mathbf{r}) d\mathbf{r} = \int d\mathbf{r} \sum_{\mathbf{k},i} w_{\mathbf{k}} f_{\sigma}(\epsilon_{i,\mathbf{k}} - \epsilon_{\text{F},\alpha(i,\mathbf{k})}) |\psi_{i,\mathbf{k}}(\mathbf{r})|^2 = N, \quad (5)$$

while maintaining specified bias voltages with respect to one reference electrode in the system:

$$\begin{aligned} \epsilon_{\text{F},1} - \epsilon_{\text{F},0} &= eV_1 \\ \epsilon_{\text{F},2} - \epsilon_{\text{F},0} &= eV_2 \\ &\vdots \\ \epsilon_{\text{F},\alpha_{\text{max}}} - \epsilon_{\text{F},0} &= eV_{\alpha_{\text{max}}}. \end{aligned} \quad (6)$$

The SCF loops are carried out in exactly the same way as in the conventional KS-DFT methods with the above occupation scheme. Notice that we have specified the bias voltage, but there is no way to calculate the accumulated charge from the above discussion. We also have no way to fix the charge on the electrodes, which means that we can carry out closed-circuit simulations, but not open-circuit ones. As noted in the Introduction, these problems can be addressed through the examination of the KS orbitals, which will be presented in the following sections.

## III. CALCULATION OF THE FREE CHARGE

To compare occupation of KS orbitals as suggested in the Introduction, we need to be able to identify which orbitals correspond to each other between calculations at different bias voltages and/or polarizations. It is not at all trivial to perform this identification automatically, and we propose the following procedure.

First, we perform a calculation of the capacitor structure that serves as the reference (i.e., the zero point) for the free charge. For example, we may take the zero-bias relaxed capacitor structure as the reference state. The KS orbitals near the Fermi level are separated into each of the electrodes based on their spatial distribution [13], and their energies and occupation are tabulated and saved in an output file. Next, we

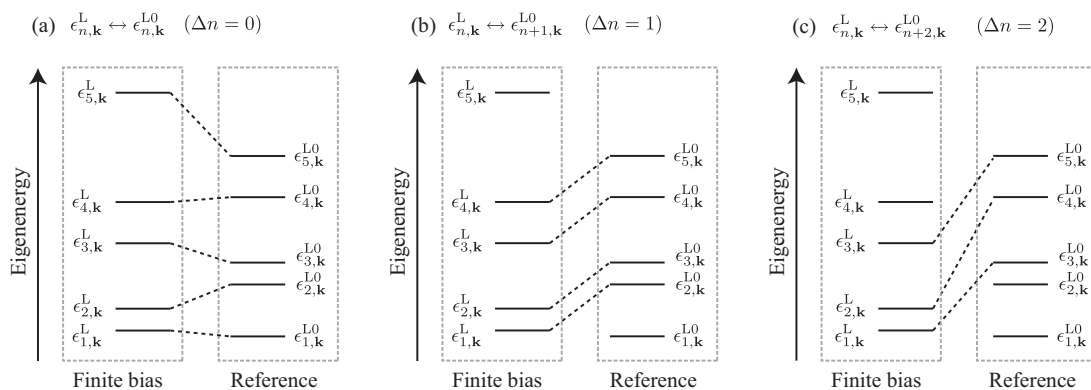


FIG. 1. Schematic of the possible ways to connect orbitals between calculations at different biases for (a)  $\Delta n = 0$ , (b)  $\Delta n = 1$ , and (c)  $\Delta n = 2$ . The dashed rectangles represent the bias window near the Fermi level in the OSA calculations. Assuming a rigid shift of the orbital energies, (b) gives the correct connection between corresponding orbitals.

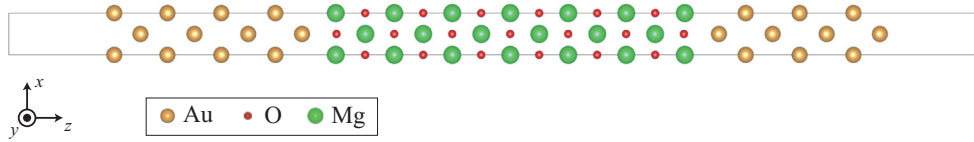


FIG. 2. (Color online) Au/MgO/Au capacitor model examined in this work. The rectangle represents the calculation cell size.

perform a calculation (which may include structural relaxation or molecular dynamics under bias) using OSA and tabulate the eigenenergies and occupations again. To connect each KS orbital to the reference eigenstate, we use the approach schematically depicted in Fig. 1: the eigenenergies within a preset window in the left electrode at each  $\mathbf{k}$  point is numbered from lowest energy to highest as  $\epsilon_{1,\mathbf{k}}^L \cdots \epsilon_{n_L,\mathbf{k}}^L$ , and those in the reference calculation is numbered similarly as  $\epsilon_{1,\mathbf{k}}^{L0} \cdots \epsilon_{n_{L0},\mathbf{k}}^{L0}$ . The possible ways to connect the reference and current eigenstates can be characterized by an integer offset value  $\Delta n$ , so that the  $n$ th eigenstate with energy  $\epsilon_{n,\mathbf{k}}^L$  is connected to the reference  $(n + \Delta n)$ th eigenstate with energy  $\epsilon_{n+\Delta n,\mathbf{k}}^{L0}$ . The eigenenergies are expected to shift by a constant as long as the amount of the free charge is small enough so that nothing drastic occurs (such as a chemical reaction at the interface) to alter the band structure of the electrodes. Thus the correct  $\Delta n$  should satisfy  $\epsilon_{1,\mathbf{k}}^L - \epsilon_{1+\Delta n,\mathbf{k}}^{L0} \simeq \cdots \simeq \epsilon_{m,\mathbf{k}}^L - \epsilon_{m+\Delta n,\mathbf{k}}^{L0} \simeq \cdots \simeq \Delta V_L$  with  $\Delta V_L$  being the shift in the electrostatic potential in the left electrode. Therefore, the correct value of  $\Delta n$  is expected to minimize

$$\max_n (\epsilon_{n,\mathbf{k}}^L - \epsilon_{n+\Delta n,\mathbf{k}}^{L0}) - \min_n (\epsilon_{n,\mathbf{k}}^L - \epsilon_{n+\Delta n,\mathbf{k}}^{L0}), \quad (7)$$

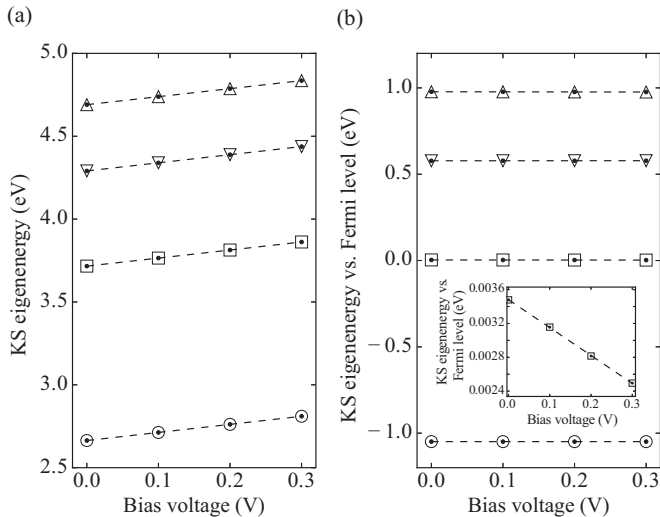


FIG. 3. Eigenenergies of the KS orbitals in the left electrode of the Au/MgO/Au model near the Fermi level plotted against the applied bias. The energies of the orbitals at the  $\mathbf{k}$ -point  $(5/12, 1/12) \cdot (\mathbf{g}_a, \mathbf{g}_b)$  are presented. In (a), the values are referred to the average potential in the calculation cell (the usual output of plane wave KS-DFT calculations under periodic boundary condition), while in (b), the values are referred to the Fermi level position in the left electrode at each bias voltage. The inset is an enlarged view of the highest (partially) occupied orbital. The dashed lines are linear fits to the data.

where we consider  $n$  values only when both  $\epsilon_{n,\mathbf{k}}^L$  and  $\epsilon_{n+\Delta n,\mathbf{k}}^{L0}$  lie within the preset bias window for the current and reference calculations, respectively. This is the criteria that we currently adopt for obtaining  $\Delta n$ , although we note that this approach is not completely foolproof; ultimately, it is recommended to make sure that the actual connections determined by the proposed algorithm are reasonable ones. Once the correspondence with the reference eigenstates is made, the free charge is calculated as

$$\Delta Q = \sum_{n,\mathbf{k}} w_{\mathbf{k}} \Delta q_{n,\mathbf{k}}, \quad (8)$$

where  $\Delta q_{n,\mathbf{k}}$  is the change in the occupation of the eigenstates near the Fermi level and  $w_{\mathbf{k}}$  is the  $\mathbf{k}$ -point weights in the Brillouin zone integration.

#### IV. TEST ON Au/MgO/Au CAPACITOR

We implemented the OSA in Vienna ab initio Simulation Package (VASP) [15,16] and performed finite-bias calculations on the Au (100)/MgO (100)/Au (100) capacitor model shown in Fig. 2. We chose the local density approximation to the exchange-correlation functional, and used the projector-augmented wave method for representing electron-ion interactions. A  $6 \times 6 \times 1$  Monkhorst-Pack  $\mathbf{k}$ -point grid was used for the calculations. Gaussian smearing of the electron occupation with a smearing width of 0.05 eV is used to speed up the convergence. The dipole correction [4] as implemented in VASP was used to cancel the interaction between adjacent unit cells.

First, we examined the change in the KS orbital eigenenergies under applied bias. Figure 3(a) shows the KS orbital eigenenergies near the Fermi level at the  $\mathbf{k}$  point  $(5/12, 1/12) \cdot (\mathbf{g}_a, \mathbf{g}_b)$  at zero bias and when positive biases of 0.1, 0.2, and 0.3 V are applied to the right electrode ( $\mathbf{g}_a$  and  $\mathbf{g}_b$  are reciprocal lattice vectors on the  $xy$  plane). The eigenenergies shift more or less by a fixed amount, meaning that the energy band structure changes very little in the

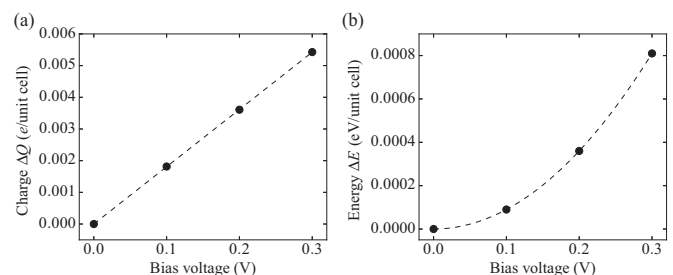


FIG. 4. Amount of free charge accumulated on the capacitor plates (a) and the increase in the energy (b) of the Au/MgO/Au capacitor due to applied bias. The dashed lines are linear fit and parabolic fit to the data for (a) and (b), respectively.

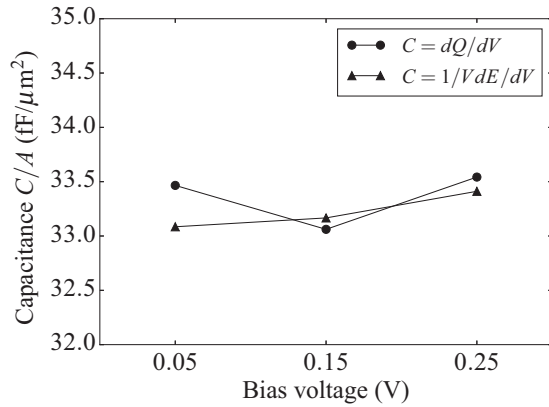


FIG. 5. Capacitance of the Au/MgO/Au capacitor evaluated from the calculated charge-voltage relation (circles) and the energy-voltage relation (triangles).

bias range examined. This shows that the assumption of the previous section is satisfied.

Figure 3(b) shows the same data as Fig. 3(a) but measured from the Fermi level in the left electrode at each of the applied biases. Very little bias dependence is observed in this plot, meaning that the Fermi level position moves only slightly with respect to the band structure (although they indeed do move as shown in the inset) due to the large density of states in the metal electrode. Thus only the KS orbitals closest to the Fermi level show changes in occupation; those higher in energy have zero occupancy, and those lower in energy are fully occupied regardless of the applied bias. Therefore, one can simply examine the change in the occupancy of KS orbitals within a preset window near the Fermi level in order to calculate the accumulated free charge. The window must be large enough to cover the region of KS eigenenergies where occupancies change between the reference and finite-bias calculations.

Figure 4(a) shows the free charge calculated using the above scheme after relaxation at 0.1, 0.2, and 0.3 V. As expected for a normal capacitor, the free charge is proportional to the applied bias voltage. The total energy shown in Fig. 4(b) shows a parabolic dependence on the bias voltage, which is also the expected behavior. As a simple sanity test, we compared the differential capacitance calculated from the charge vs bias  $C = dQ/dV$  and energy vs bias  $C = 1/V dE_{\text{KS}}/dV$  (see Ref. [13] for derivation). As shown in Fig. 5, the differences in results are within 2% of the obtained capacitance values, attesting to the soundness of the procedure outlined here.

## V. CONSTANT-CHARGE CALCULATION: ZERO-POLARIZATION STATE OF SrRuO<sub>3</sub>/BaTiO<sub>3</sub>/SrRuO<sub>3</sub> CAPACITOR

Since we are now able to calculate the free charge with respect to a reference calculation of a metal-insulator-metal capacitor, it is relatively straightforward to implement a constant-charge method. That is, at each self-consistent field (SCF) step in the KS-DFT-based OSA calculation, we solve for the bias voltage  $V$  between the electrodes that results in the preset free charge  $\Delta Q$  vs the reference system. We note that the scheme would fail if the states near the Fermi level change too much between SCF steps, so the constant-charge calculations are started by reusing the KS wave functions and electron density of the reference state. A small enough  $\Delta Q$  value and careful mixing of the electron density between SCF steps was found to be necessary to obtain stable convergence to the ground state at constant free charge.

To test our constant-charge implementation in VASP, we performed calculations on the SrRuO<sub>3</sub>/BaTiO<sub>3</sub>/SrRuO<sub>3</sub> (SRO/BTO/SRO) model shown in Fig. 6. The BTO slab is thicker than the critical thickness for monodomain ferroelectricity [17] so there is nonzero spontaneous polarization. We performed structural relaxation of this capacitor structure while fixing the free charge, which corresponds to fixing the electric displacement  $D$  [14]. This allows the examination of the region of  $D$  which is thermodynamically unstable at constant bias voltage, such as a ferroelectric near zero polarization. We stress that such calculations are not possible in the original orbital-separation approach of Ref. [13], which could only fix the voltage but not the electric displacement. Although such zero-polarization states are not accessible in usual experiments where voltage is regulated, the calculations are very useful for examining the strength of the ferroelectric instability [14]. Furthermore, a recent experimental report claims that information from this region can be extracted from the transient current and voltage during polarization switching [18].

We started from the zero-bias left-polarized structure shown in Fig. 6 and performed relaxation at decreasing free charge  $\Delta Q$  values (electrons were removed from the left electrode and added to the right) until the zero-polarization centrosymmetric BTO structure was reached. Figure 7(a) shows the  $z$  displacement of the Ba ions vs the O ions in the central BaO layer [Fig. 6(b)]. We find that the zero-polarization state is reached when  $\sim 0.265$  electrons per unit cell is transferred from the left electrode to the right electrode. The voltage vs

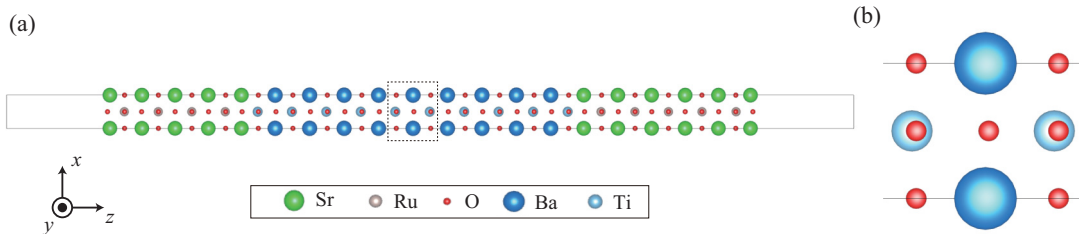


FIG. 6. (Color online) (a) Calculation cell of the SRO/BTO/SRO capacitor model examined in this work and (b) an expanded view of the region surrounded by the dashed rectangle. The BTO slab shows spontaneous polarization towards the left (cations in each layer are displaced to the left, while anions are displaced to the right).

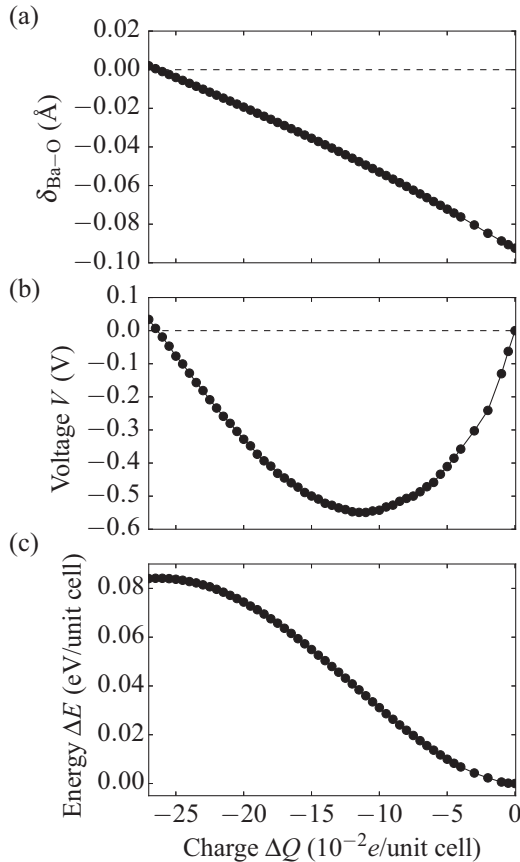


FIG. 7. (a) Cation-anion displacement  $\delta_{\text{Ba-O}}$ , (b) voltage  $V$ , and (c) the total energy  $\Delta E$  of the SRO/BTO/SRO capacitor after relaxation at fixed charge  $\Delta Q$ . Note that  $\Delta Q = 0$  corresponds to the situation where the BTO slab is spontaneously polarized towards the left as in Fig. 6(b).

free charge [Fig. 7(b)] shows the S-shape nonlinearity and the energy vs free charge [Fig. 7(c)] shows the double-well structure characteristic of ferroelectric materials. Moreover, the maximum in the energy, zero polarization, and zero voltage all coincide at the same  $\Delta Q$  value of  $\sim -0.265e/\text{unit cell}$ , which is the expected behavior attesting to the reliability and accuracy of our scheme. Additionally, we calculated the local inverse permittivity profile at zero polarization (Fig. 8) by calculating  $d\bar{E}(z)/dD$ , where  $\bar{E}$  is the  $xy$ -plane-averaged and nanosmoothed electrostatic field in the direction perpendicular to the interface, and  $D = Q/A$  is the electric displacement (which is equal to the free charge density). The nanosmoothing has been performed using convolution by a Gaussian kernel [19]. A decrease in the local permittivity is seen at the interface of SRO and BTO (the so-called dead layer effect), and the inverse permittivity converges to the value of  $-0.022$  in the middle of the BTO slab in good agreement with a previous work using maximally localized Wannier functions (MLWFs) to perform fixed- $D$  simulations [20]. We note, in passing, that although the OSA gives virtually identical results with the MLWF approach for parallel-plate capacitors, we may just as easily employ the OSA to treat non-parallel-plate capacitor geometries. Doing the same in the MLWF approach gives rise to complications otherwise absent in the parallel-plate case.

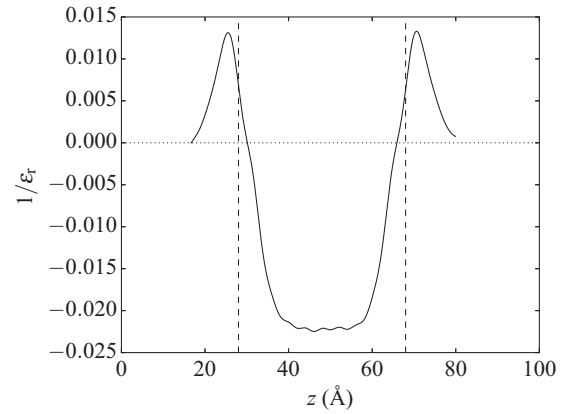


FIG. 8. Inverse permittivity profile of the SRO/BTO/SRO capacitor at the zero-polarization state. The dashed vertical lines indicate the interfacial SrO layers.

This is due to the fact that although one-shot Wannierization is possible in one dimension, the same is not possible in two or more dimensions; iterative minimization of the spread functional as well as specification of sensible initial guesses are required in those cases, requiring user interaction in the simulation process [11].

## VI. CONCLUSION

In this work, we extended the orbital-separation approach (OSA) to calculate the free charge accumulated on a capacitor under finite bias. Using the calculated free charge and the energy of the capacitor, we can calculate the grand potential of the system from Eq. (1). This means that it is now possible to evaluate the stability of electrochemical interfaces under bias from the energetics obtained from first principles by using the OSA. Furthermore, we developed a constant-charge version of OSA and tested its use on the thermodynamically unstable zero-polarization state of a ferroelectric capacitor. We confirmed the reliability and robustness of the method through the examination of the relationship between the polarization, voltage, and the ferroelectric double-well energy structure. Summarizing the above, the applicability of the OSA has been extended to include both open-circuit and closed-circuit situations in experiments and device operation. The OSA now provides access to forces acting on ions as well as the grand potential that allows for examination of the thermodynamics of metal/insulator/metal systems of arbitrary geometry under finite bias as long as there is negligible current flowing between electrodes. This would further facilitate the simulation of novel devices in complex geometries, e.g., switching and/or memory devices utilizing multiferroic materials with multiple electrodes.

## ACKNOWLEDGMENTS

The calculations were performed on the SGI Altix 3800EX system at the Institute for Solid State Physics, the University of Tokyo. S.K. is supported by Grant-in-Aid for Young Scientists (B) (Grant No. 15K20953) by Japan Society for the Promotion of Science (JSPS). S.W. is supported by Grant-

in-Aid for Scientific Research(B) (Grant No. 15H03561) by JSPS. Atomic structure figures were created using VESTA

visualization software [21]. The data analysis and plotting were performed using SciPy [22] and matplotlib [23].

- 
- [1] P. Hohenberg and W. Kohn, *Phys. Rev.* **136**, B864 (1964).
  - [2] W. Kohn and L. J. Sham, *Phys. Rev.* **140**, A1133 (1965).
  - [3] J. Neugebauer and M. Scheffler, *Phys. Rev. B* **46**, 16067 (1992).
  - [4] L. Bengtsson, *Phys. Rev. B* **59**, 12301 (1999).
  - [5] Y. Gohda, Y. Nakamura, K. Watanabe, and S. Watanabe, *Phys. Rev. Lett.* **85**, 1750 (2000).
  - [6] N. Nakaoka, K. Tada, S. Watanabe, H. Fujita, and K. Watanabe, *Phys. Rev. Lett.* **86**, 540 (2001).
  - [7] M. Brandbyge, J.-L. Mozos, P. Ordejón, J. Taylor, and K. Stokbro, *Phys. Rev. B* **65**, 165401 (2002).
  - [8] K. Burke, R. Car, and R. Gebauer, *Phys. Rev. Lett.* **94**, 146803 (2005).
  - [9] M. Otani and O. Sugino, *Phys. Rev. B* **73**, 115407 (2006).
  - [10] K. Uchida, H. Kageshima, and H. Inokawa, *Phys. Rev. B* **74**, 035408 (2006).
  - [11] M. Stengel and N. A. Spaldin, *Phys. Rev. B* **75**, 205121 (2007).
  - [12] B. Lee, C.-K. Lee, S. Han, J. Lee, and C. S. Hwang, *J. Appl. Phys.* **103**, 024106 (2008).
  - [13] S. Kasamatsu, S. Watanabe, and S. Han, *Phys. Rev. B* **84**, 085120 (2011).
  - [14] M. Stengel, N. A. Spaldin, and D. Vanderbilt, *Nat. Phys.* **5**, 304 (2009).
  - [15] G. Kresse and J. Furthmüller, *Phys. Rev. B* **54**, 11169 (1996).
  - [16] G. Kresse and D. Joubert, *Phys. Rev. B* **59**, 1758 (1999).
  - [17] J. Junquera and P. Ghosez, *Nature (London)* **422**, 506 (2003).
  - [18] A. I. Khan, K. Chatterjee, B. Wang, S. Drapcho, L. You, C. Serrao, S. R. Bakaul, R. Ramesh, and S. Salahuddin, *Nat. Mater.* **14**, 182 (2014).
  - [19] F. Giustino and A. Pasquarello, *Phys. Rev. B* **71**, 144104 (2005).
  - [20] M. Stengel, D. Vanderbilt, and N. A. Spaldin, *Nat. Mater.* **8**, 392 (2009).
  - [21] K. Momma and F. Izumi, *J. Appl. Crystallogr.* **41**, 653 (2008).
  - [22] E. Jones, T. Oliphant, P. Peterson *et al.*, “SciPy: Open source scientific tools for Python,” <http://www.scipy.org> (2001–).
  - [23] J. D. Hunter, *Comput. Sci. Eng.* **9**, 90 (2007).